Correspondence

Design and Implementation of a Smartphone-Based Portable Ultrasound Pulsed-Wave Doppler Device for Blood Flow Measurement

Chih-Chung Huang, Po-Yang Lee, Pay-Yu Chen, and Ting-Yu Liu

***Abstract*—Blood flow measurement using Doppler ultrasound has become a useful tool for diagnosing cardiovascular diseases and as a physiological monitor. Recently, pocket-sized ultrasound scanners have been introduced for portable diagnosis. The present paper reports the implementation of a portable ultrasound pulsed-wave (PW) Doppler flowmeter using a smartphone. A 10-MHz ultrasonic surface transducer was designed for the dynamic monitoring of blood flow velocity. The directional baseband Doppler shift signals were obtained using a portable analog circuit system. After hardware processing, the Doppler signals were fed directly to a smartphone for Doppler spectrogram analysis and display in real time. To the best of our knowledge, this is the first report of the use of this system for medical ultrasound Doppler signal processing. A Couette flow phantom, consisting of two parallel disks with a 2-mm gap, was used to evaluate and calibrate the device. Doppler spectrograms of porcine blood flow were measured using this stand-alone portable device under the pulsatile condition. Subsequently, *in vivo* portable system verification was performed by measuring the arterial blood flow of a rat and comparing the results with the measurement from a commercial ultrasound duplex scanner. All of the results demonstrated the potential for using a smartphone as a novel embedded system for portable medical ultrasound applications.**

I. Introduction

Doppler ultrasound is widely used in medicine for assessing blood flow and diagnosing various cardiac and blood vessel diseases in the central and peripheral circulation because it is noninvasive and capable of real-time measurement [1]–[3]. Blood flow information can be regarded as an index for monitoring physiological functions, as well as blood pressure and blood oxygenation. Doppler ultrasound has been also used to measure blood flow in blood rheology [4]–[6], sports medicine [7]–[9], and sleep medicine studies [10], [11]. For instance, some investigations have indicated that the arterial flow velocity was different after exercise or during sleep apnea. However, it is not convenient to use a commercial ultrasound duplex scanner for Doppler measurements during exercise or sleep, even though some small portable ultrasound scanners are available. In addition to the size of the system, another consideration is the need for the ultrasound probe to be held by an operator. In other words, a portable Doppler ultrasound device with a surface probe is needed for these applications [12].

Both the principles and the signal processing details of a pulsed-wave (PW) Doppler system have been introduced in previous papers and textbooks [13]–[20]. However, the performance and miniaturization of a PW system can be significantly improved by using novel electronic components. Another important issue for a portable Doppler ultrasound device is the need for a real-time spectral analyzer. Most studies have used the DSP and/or FPGA chip to calculate the Doppler spectrograms from flowing blood [21]–[23]. However, some additional components are needed such as an RF and/or audio analog-to-digital converter (ADC), on-board data memory, programmable timer, and LCD graphic display module and its control circuit (or the connector module for a laptop display) [24], [25]. The idea of using a smartphone to replace these complex modules is proposed in this study. The smartphone can accordingly be regarded as a novel embedded system that contains all of the required units for audio signal and image processing. Because a smartphone offers advanced computing ability and a high-quality color display, the Doppler signals from a PW analog system can be analyzed conveniently for display or storage in real time. Ultrasound imaging with a smartphone was performed using a USB ultrasound probe by Richard *et al.* [26]. The transducer elements and electronic circuits were implemented on a small circuit board inside the probe. Even though this smartphone-based ultrasound device could provide B-mode imaging, it did not have a Doppler flow function and the design conflicts with our expectation that the probe should not be held by an operator.

The main purpose of this study was to develop a portable PW Doppler flowmeter based on an external electronic board and a smartphone for the real-time measurement of blood flow velocity during physical exercise and postural changes. A 10-MHz surface transducer with good attachment to the skin was designed for transmitting and receiving ultrasound signals. The Doppler shift signals were obtained using analog circuits. Subsequently, the Doppler signals were digitized by the built-in ADC of the smartphone via a microphone jack. Doppler spectrum processing was implemented through a program written on the Android platform (Google Inc., Mountain View, CA) for a stand-alone smartphone. Both Doppler signals and Doppler spectrograms can be stored on a built-in memory card, as well as displayed in real time on the touch screen. The blood flow velocity measurement accuracy was tested using a Couette flow phantom *in vitro*. Finally, the arterial blood flow of a rat was measured *in vivo* to verify the performance of the smartphone-based portable PW Doppler ultrasound device.

Manuscript received August 16, 2011; accepted November 2, 2011.

The authors are with the Department of Electrical Engineering, Fu Jen Catholic University, Taiwan (e-mail: j648816n@ms23.hinet.net).

P.-Y. Lee and T.-Y. Liu are also with the Graduate Institute of Applied Science and Engineering, Fu Jen Catholic University, Taipei, Taiwan.

Digital Object Identifier 10.1109/TUFFC.2012.2171

0885–3010/$25.00 © 2012 IEEE

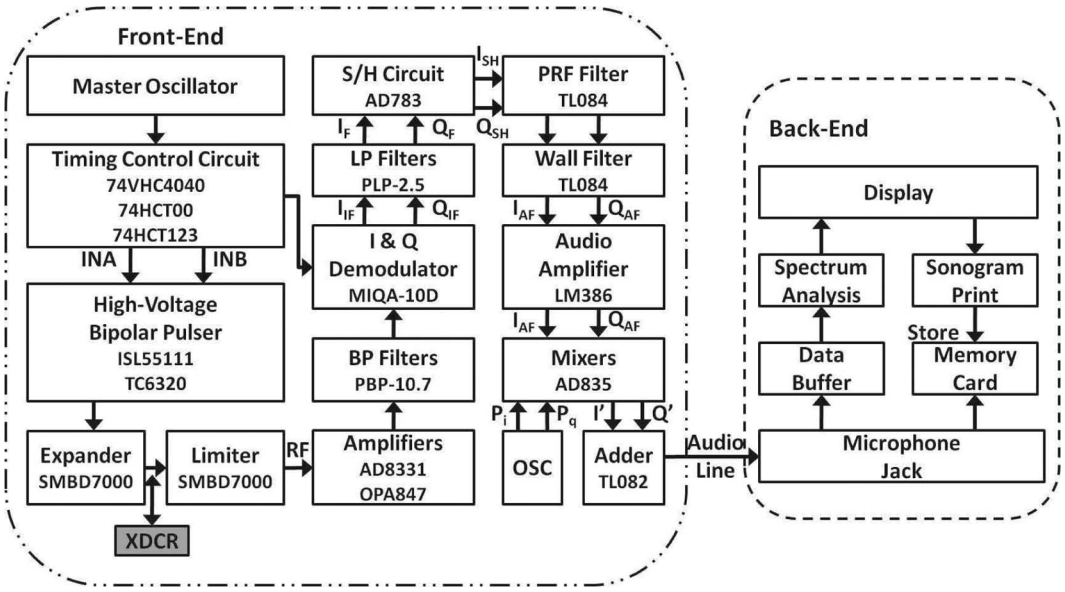

Fig. 1. Block diagram of smartphone-based portable pulsed-wave Doppler device. The part numbers of used ICs are shown in blocks.

II. System Description

Fig. 1 shows the block diagram of the portable smartphone-based PW Doppler ultrasound device. The system included two independent modules: a low-cost analog circuit for Doppler shift signal processing, as shown in the dash-dotted-line box (front-end), and a smartphone for Doppler spectrogram analysis, which is shown in the dashed-line box (back-end). The main circuits of the front end include a pulse repetition frequency (PRF) timing controller, bipolar pulser and receiver, in-phase and quadrature-phase (I/Q) demodulation circuits, S/H circuits, PRF filters, wall filters, audio amplifiers, and Weaver receiver processor. These electronic circuits are described in detail in the following sections.

The timing controller was based on transistor–transistor logic (TTL) circuits and provided matched trigger signals for the bipolar pulser and S/H gating, as shown in Fig. 2. A 40-MHz crystal oscillator was used to generate a stable clock. A 10-MHz rectangular clock (A) and PRF clock (B) were obtained by dividing the 40-MHz clock using a 12-bit counter. Subsequently, the duty cycle of the PRF pulse (C) was adjusted, based on the anticipated number of bipolar pulser cycles. A 50-ns delay PRF pulse (D) was also obtained by regulating the accessory RC components. Two logic control inputs, INA (E) and INB (F), were needed for the bipolar pulser. An S/H gating trigger (G) was also generated by delaying the PRF pulse (C), with a variable range gating of 0.5 to 25 μs. The logic signals (E and F) and S/H gating trigger (G) were fed to the bipolar pulser and S/H circuits, respectively. A high-speed, high-voltage MOSFET pairs, was used to generate a bipolar pulse [27], [28]. A high-speed MOSFET driver was placed in front of the MOSFET pair to boost the TTL voltage from 5 V to 12 V. The tone burst then excited the transducer via a protection circuit (expander).

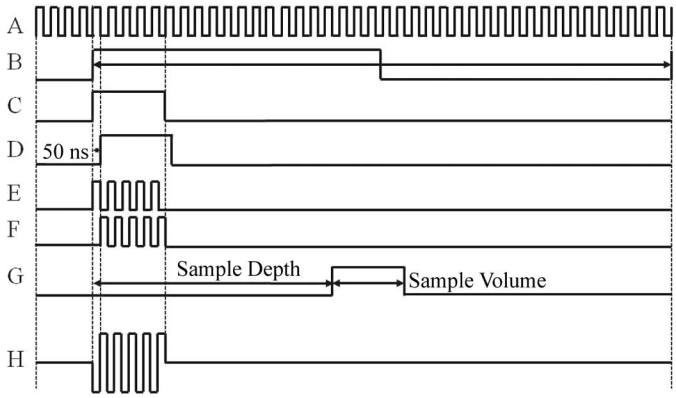

Fig. 2. Timing sequences of signals in timing controller circuits, bipolar pulser, and sample-and-hold circuits.

The output of the bipolar pulser drove a 50-Ω load; the maximum output voltage of this system was 100 Vpp and the −6-dB bandwidth of bipolar signal was 25%. The RPF can be changed by switching the divider. These circuits are pin-compatible so no wiring change is needed. In this system, the PRF can be changed to 9.25, 18.5, 39, and 78 kHz. A PRF of 39 kHz and 5 cycles were used for the bipolar pulser (H) in present study. The backscattering signals from flowing blood were amplified by a two-stage amplifier. A total gain of 80 dB was achieved using this two-stage amplifier. A 50-dB gain was set for present measurements. An electronic limiter was placed in front of the preamplifier to ensure that the large excitation signal did not enter the preamplifier. Subsequently, a band-pass filter with a −3-dB bandwidth from 8.9 to 12.7 MHz was used to remove noise signals.

The direction of blood flow was determined by I/Q demodulation, and the local flow velocity was obtained using S/H circuits. The I/Q demodulation circuits included multipliers and low-pass filters. The echoes from the re-

TABLE I. THE SPECIFICATIONS OF ANALOG PULSED-WAVE DOPPLER FLOWMETER.

Center operation frequency	10 MHz
Pulse repetition frequency (PRF)	9.25, 18.5, 39, and 78 kHz
Transmitted pulse duration	0.5 μs
Output voltage	±50 V
Range gate (adjustable)	0.5 to 25 μs (0.4 to 19 mm)
Wall filter	250 Hz

ceiver were fed directly to an I/Q demodulator. After the multiplication of the backscattering signal and the carrier signal, the demodulated intermediate frequency (IF) signals, I_{IF} and Q_{IF}, were low-pass filtered to remove the high-frequency carrier signals and reduce noise using two commercial low-pass filters with a −3-dB cutoff-frequency of 2.75 MHz. The output signals from the demodulation circuits were sampled at a variable depth (in the range from 0.4 to 19 mm) by S/H circuits. For example, the selected depth was 8 mm for measuring rat blood flow velocity in present study. The sampling frequency of the S/H circuits was consistent with the PRF, and an RC timing delay circuit was used to adjust the range-gate, with the sample volume equal to the transmitted pulse duration of 0.5 μs. Subsequently, an active 8th-order low-pass filter was used to remove the replica at PRF, which had a −3-dB cutoff frequency adjusted according to the timing control circuits. An active 8th-order wall filter was then used to remove the low-frequency clutter signals. Finally, the two-channel baseband Doppler frequency signals, I_{AF} and Q_{AF}, were amplified using audio amplifiers. Because most smartphones only have one channel for audio input signals, the Weaver receiver technique (WRT) was used for determining the direction of blood flow [22]. Both Doppler frequency signals, I_{AF} and Q_{AF}, are mixed with quadrature signals from a oscillator which has a pilot frequency of 12 kHz. After adding I′ and Q′, only one built-in ADC is required for directional determination of flow. The directional output signals were then fed to the smartphone for Doppler spectrogram analysis. The pilot frequency can be removed numerically by normalizing the baseline of Doppler spectrogram to 0 Hz [22]. The specifications of this analog PW Doppler flowmeter are listed in Table I.

Because the battery of the smartphone was depleted rapidly during the computing and display of Doppler spectrograms, especially when the high-quality color level capacitive touch screen is working, a rechargeable three-cell lithium-ion battery was used as the power supply for both smartphone and analog circuits. The output voltage and capacity of this series battery were 12.6 V and 2200 mAh, respectively. Two DC-to-DC regulated dual-output converters (DCW05A-12 and DCW05A-05, Mean-well Taiwan, New Taipei, Taiwan) were used to provide optimal dual power of ±12 and ±5 V to all analog components. Two miniature and ultra-low ripple (<50 mVpp) high-voltage DC-to-DC converters (PCS01–05N050 and PCS01–05P050, 3Gold Electronics Co., Ltd., Hsin-Chu, Taiwan) were used together to supply the high voltage

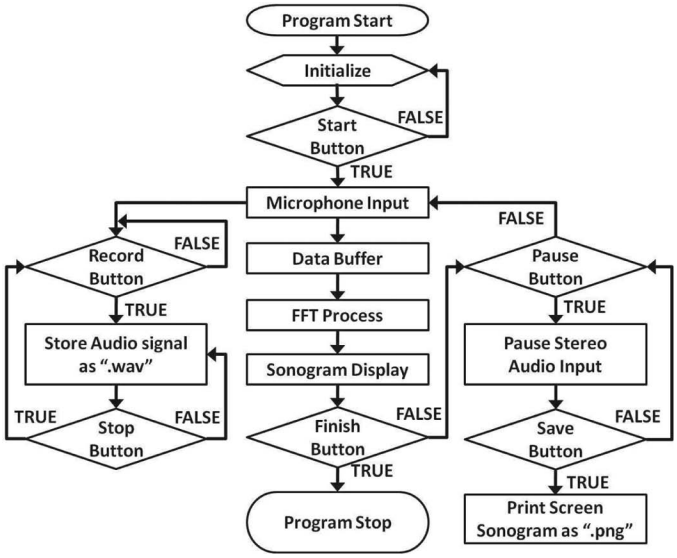

Fig. 3. Flowchart of Doppler spectrogram analysis on Android platform.

(±50 V) to the bipolar pulser. A four-layer well-designed printed circuit board (PCB) was considered to provide better ground coupling and power distribution. Clean power supplies were needed to reduce any possible noise jamming. The beads and capacitors were placed as close as possible to the power pins of the chips, and all of the signal sources were well shielded and impedance matched. In the present study, the system can work for 5 h after a full charge of the external battery.

Fig. 3 shows a flowchart of the Doppler spectrogram analysis that was performed on a smartphone (Desire, HTC Co., Taoyuan, Taiwan). The software implementation was carried out on the Android 2.2 (Froyo) Developer which is based on Java programming language (Sun Microsystems Inc., Santa Clara, CA). The Android Development tools (ADT) was plugged into the Eclipse (Eclipse Foundation Inc., Ottawa, ON, Canada) integrated development environment (IDE) which provides an integrated development environment for Android applications. The Java programming was compiled by the Android software development kit (SDK) and an Android package file (*.apk) was subsequently created. The Android package file was installed on the smartphone for Doppler spectrogram analysis. The sampling frequency of the built-in ADC was set at 48 kHz. After initializing the program, a byte buffer was created to capture the directional baseband Doppler signals. Subsequently, the Doppler signals were converted into a byte array. The directional Doppler signals were segmented using a temporal window of 480 sample points. The Doppler spectrum was obtained using the fast Fourier transform (FFT), and the overlap window between consecutive processing was 50%. A Hamming windowed signal for each segment was taken for 512 points FFT. The Doppler spectrogram corresponding to each temporal window was then displayed in 8-bit self-color level on the capacitive touch screen with pinch-to-zoom capability. The data processing can be stopped at any time, and the raw data of direc-

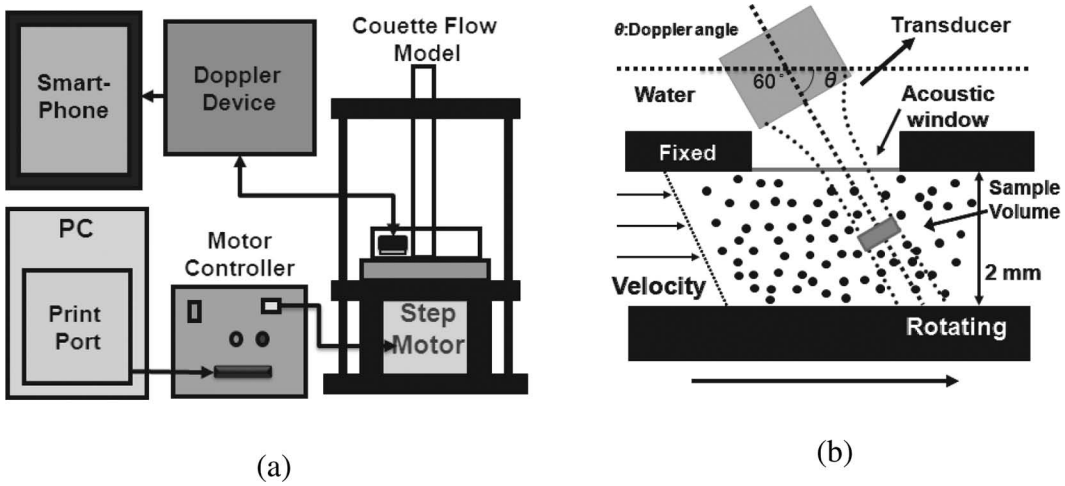

Fig. 4. Couette flow phantom (a) and measurement setup (b).

tional Doppler signals and Doppler spectra can be stored on the built-in memory card (microSD). A 4-GB microSD card was used in present system.

III. System Verification

Both *in vitro* blood flow velocity measurement and *in vivo* testing were carried out to verify the performance of the PW Doppler flowmeter. The *in vitro* testing was performed using a Couette flow phantom, as shown in Fig. 4(a). A porcine blood sample was placed in the space between two parallel disks, one of which was moving relative to the other. The gap between these two parallel disks was 2 mm. The rotating disk was fixed to a stepper motor (RK564-T3.6, Oriental Motor, Tokyo, Japan) driven by a motor controller. A circular acoustic window with a diameter of 13 mm was created on the upper disk. A polymethylpentene film (TPX, Mitsui, White Plains, NY) was used to cover this acoustic window, which allowed most of the ultrasound energy to be transmitted to and received from the blood. The ultrasonic transducer was immersed in distilled water, and positioned at a Doppler angle of 60° to the acoustic window, as shown in Fig. 4(b). For all of the measurements, the sample volume was located near the center stream. For pulsatile flow experiments, the stroke rate was set to 15 beats/min (BPM) at a peak flow velocity of 120 cm/s by controlling the rotating speed of the Couette flow phantom. All of the experiments were performed at a room temperature of 25°C.

Although animal experiments must be performed before we can use this device for human testing, a transducer design was considered for human applications. A 10-MHz surface ultrasonic transducer (PMN-PT) was fabricated (NIH Resource on Medical Ultrasonic Transducer Technology, University of Southern California, Los Angeles, CA) for *in vivo* experiments. This transducer has a thickness of 1.0 cm and an aperture diameter of 0.4 cm. The *in vivo* experiments were performed on a Wistar rat (Laboratory Animal Center, National Taiwan University College of Medicine, Taipei, Taiwan). The protocol for this animal experiment was approved by the Institutional Animal Care and Use Committee of Fu-Jen Catholic University. The rat was anesthetized with pentobarbital sodium (SCI Pharmtech Inc., Taoyuan, Taiwan) diluted in saline to 45 mg/mL and injected intraperitoneally at a dosage of 1 mL/kg body weight. Subsequently, the chest of the rat was shaved and cleaned with a chemical hair remover. The transducer could be well attached to the skin using medical tape. Portable system verification was performed by measuring the arterial blood flow velocity of the rat and then comparing with the Doppler spectrogram measurements from a commercial duplex scanner (t3000, Terason, Burlington, MA) with a 12L5 linear array probe.

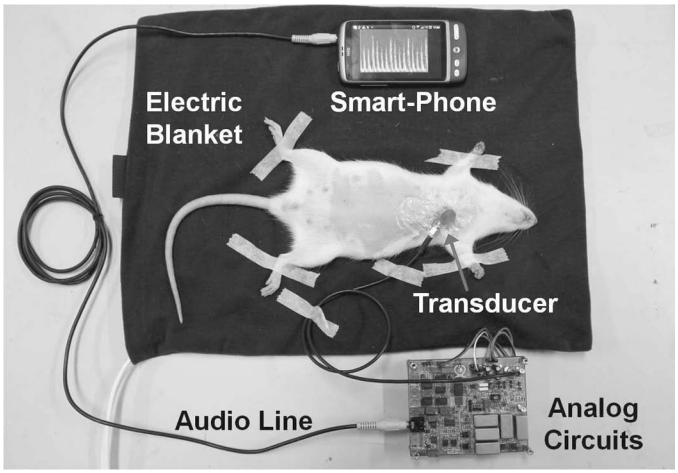

Fig. 5. Illustration of animal experiment and the prototype of portable pulsed-wave Doppler device. The transducer was well attached to the skin by medical tape.

IV. Results and Discussion

Fig. 5 shows the prototype of the portable device, which consists of an analog circuit PCB (front-end) and smartphone (back-end). The PCB includes all of the electron-

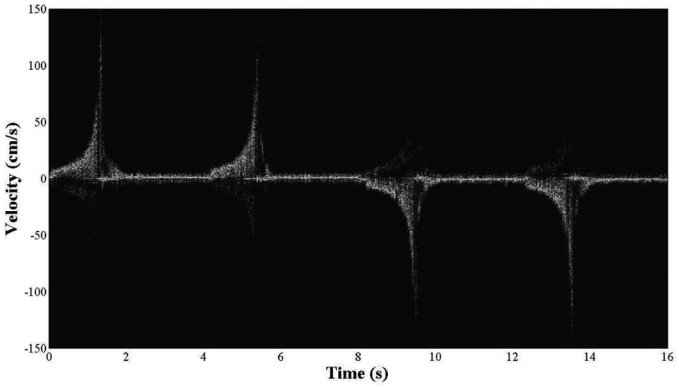

Fig. 6. Doppler spectrogram of flowing blood from Couette flow phantom.

ics needed for a complete PW Doppler flowmeter; a user interface running on the smartphone can show a Doppler spectrogram in real time. The size of the front-end (10 × 8 × 2 cm) allows us to stack it with a smartphone for portable application. In addition to real-time capability, both the Doppler signal raw data and Doppler spectrograms can be recorded on the built-in memory card for off-line processing. The main advantage of this design is the ability to attach this front-end device to most smartphones that allow the user to install and execute advanced applications. Although, to the best of our knowledge, this is the first report on the use of the Android platform for a medical ultrasound Doppler application, a similar application program can be executed on other smartphone operating system platforms such as Symbian (Accenture, Dublin, Ireland), IOS (iPhone; Apple Inc., Cupertino, CA), and Windows Phone (Microsoft Corp., Redmond, WA). Although the hardware requirement was not tested systematically in this report, the application program can be executed on a 500-MHz processor with 384 MB of RAM, which is within the specifications of most modern smartphones. In addition, only a one-channel audio jack input is needed because the WRT was used in analog circuits to determine the flow direction.

The result of the *in vitro* blood flow verification is shown in Fig. 6. The blood flow velocity of the Couette flow phantom was accelerated to 120 cm/s at a stroke rate 15 BPM. The measured result of the Doppler spectrogram was in good agreement with the default values of the flow phantom. The temporal resolution of the Doppler spectrogram was 10 ms, with a temporal overlap of 50% (Each Doppler spectrum was calculated from 50% old and 50% new samples of Doppler signal). The raw data for the Doppler information from the smartphone memory card were displayed off-line using Matlab (The MathWorks Inc., Natick, MA). A peak flow velocity of 120 cm/s was set to simulate the maximum velocity of human arterial blood flow. In addition, the direction of blood can be measured in this portable device, as shown in Fig. 6. The loss of the Doppler spectrogram at a lower velocity may be attributed to the high-pass nature of the wall filter. However, the details of the blood flow velocity were observed

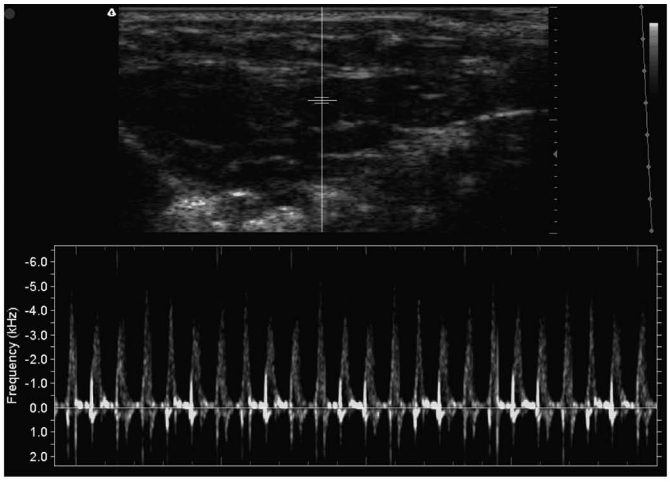

(a)

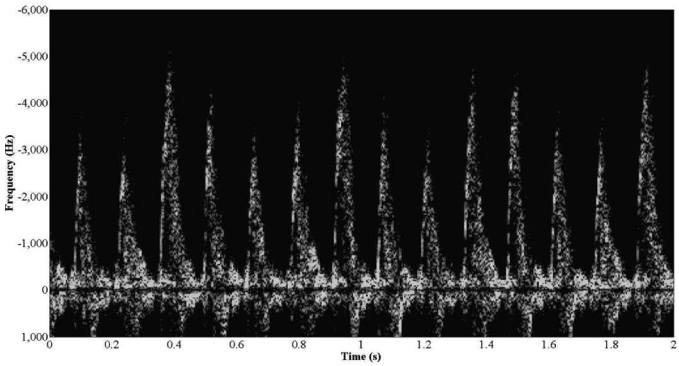

(b)

Fig. 7. Measurements of Doppler spectrogram from rat arterial blood flow using (a) a commercial scanner and (b) portable pulsed-wave Doppler device.

during the acceleration. All of the results showed the high performance and accuracy of this PW Doppler device.

The *in vivo* verification was performed by measuring the Doppler spectrogram of arterial blood flow and comparing with the measurement from a commercial scanner, as shown in Fig. 7. Both measurements were carried out for a rat at the same position. The B-mode image shows that the diameter of the artery was approximately 3 mm, with a depth of 0.8 to 1.0 cm. The sample volume (0.5 mm) for the PW Doppler spectrogram was located at the central stream, as shown in Fig. 7(a). The negative and positive frequencies indicated the flow direction. Similar measured Doppler spectrogram results were obtained from the portable PW Doppler device, as shown in Fig. 7(b). The measured average time intervals between two consecutive peak flows for commercial scanner and prototype were approximately 0.155 and 0.143 s, respectively. The zero Doppler frequency was observed in Fig 7(b) because a wall filter of 250 Hz was used for rat experiments. The slight difference of heart rate in Fig. 7 may be attributed to the depth of anesthesia being changed during the experimental measurements. However, a slight noise was observed in this Doppler spectrogram compared with the

Fig. 8. Future application of the portable Doppler device for human blood flow monitor.

commercial scanner. This may be attributed to using only the FFT algorithm. We did not apply any digital filtering in the audio signal processing because it may increase the processing time of the Android system. Another factor may be the poor quality of the RF signals that were received from the rat blood because of the high ultrasonic attenuation and reflection of the chest bone. However, the results still show the potential for using this device for *in vivo* measurements. The influence of bone on ultrasound penetration can be ignored when measuring human carotid arteries. Fig. 8 shows the future application for this portable Doppler device. The surface transducer is securely attached to the neck, and the portable Doppler device is strapped to the arm. Blood flow information can then be obtained during physical exercise and postural changes.

Another advantage of this smartphone-based Doppler device is the telemetry. A modern smartphone provides wireless communication capability, such as 3rd generation mobile telecommunications (3G), Wi-Fi, and bluetooth. The Doppler information could easily be transmitted to remote servers via these built-in wireless technologies without any additional components. In addition, this device could be used on ambulances, for which an application could combine the blood flow information with their location, as monitored by the global positioning system (GPS). All of these applications provide the advantage of using a smartphone as a novel embedded system for portable medical applications. Because the Doppler angle is important for blood flow velocity measurements, an angled lens in front of the transducer can be designed to fix the Doppler angle in real applications. In addition, the B-mode imaging can be applied to assess the Doppler angle before we attach the surface ultrasonic transducer on the neck. Currently, the sample depth was adjusted by a variable resistor. Automatic function will be considered in future works. This device may provide useful information for early detection of blood flow change; however, the user still needs professional diagnosis from a physician. Certainly, more study is required, in terms of the accuracy, stability, and safety, before we can really apply the current device for *in vivo* human applications.

V. Conclusion

The electronics for a smartphone-based portable PW Doppler device were described in this paper. A 10-MHz surface transducer was designed for measuring the blood flow velocity without the need for an operator-held probe. The Doppler shift signals were obtained by hardware processing via analog circuits. The Doppler spectrogram was computed on a smartphone using an Android application program. In this system, both the signal and spectrogram can be stored and displayed in real time. The system performance was verified using a Couette flow phantom under the pulsatile condition. A maximum flow velocity of 120 cm/s could be measured by this device, and the details of blood flow acceleration were observed continuously. An *in vivo* experiment was carried out by measuring the arterial blood flow of a rat. Although the Doppler spectrogram was influenced slightly by noise, the result was in a good agreement with the measurement from a commercial scanner. Future work will apply this portable device to a human, and the wireless communication capability should be addressed for telehealth applications. In addition, a medium-complexity field-programmable gate array (FPGA) should be considered for integrating all needed signal processing and reducing the cost. With such an approach, the board could be smaller and lead to all the obvious benefits of digital realizations.

Acknowledgments

The authors gratefully acknowledge Dr. K. K. Shung and Dr. Q. Zhou for assistance with transducer fabrication, and Dr. J. J. Wang for assistance with the animal experiments.

References

[1] K. K. Shung, *Diagnostic Ultrasound: Imaging and Blood Flow Measurements*. Boca Raton, FL: CRC Press, 2006.

[2] T. L. Szabo, *Diagnostic Ultrasound Imaging: Inside Out*. Burlington, MA: Elsevier Academic, 2004.

[3] D. W. Baker, S. A. Rubenstein, and G. S. Lorch, "Pulsed Doppler echocardiography: Principles and application," *Am. J. Med.*, vol. 63, no. 1, pp. 69–80, 1977.

[4] C. C. Huang, S. H. Wang, and P. H. Tsui, "In vitro study on the assessment of blood coagulation and clot formation using Doppler ultrasound," *Jpn. J. Appl. Phys.*, vol. 44, no. 12, pp. 8727–8732, 2005.

[5] C. C. Huang, "Cyclic variations of high-frequency ultrasonic backscattering from blood under pulsatile flow," *IEEE Trans. Ultrason. Ferroelectr. Freq. Control*, vol. 56, no. 8, pp. 1677–1688, 2009.

[6] C. C. Huang, "Detecting spatial variations of erythrocytes by ultrasound backscattering statistical parameters under pulsatile flow," *IEEE Trans. Biomed. Eng.*, vol. 58, no. 5, pp. 1163–1171, 2011.

[7] L. G. Jørgensen, G. Perko, and N. H. Secher, "Regional cerebral artery mean flow velocity and blood flow during dynamic exercise in humans," *J. Appl. Physiol.*, vol. 73, no. 5, pp. 1825–1830, 1992.

[8] G. Hellström, W. Fischer-Colbrie, N. G. Wahlgren, and T. Jogestrand, "Carotid artery blood flow and middle cerebral artery blood flow velocity during physical exercise," *J. Appl. Physiol.*, vol. 81, no. 1, pp. 413–418, 1996.

[9] Z. L. Jiang, H. Yamaguchi, A. Takahashi, S. Tanabe, N. Utsuyama, T. Ikehara, K. Hosokawa, H. Tanaka, Y. Kinouchi, and H. Miyamoto, "Blood flow velocity in the common carotid artery in humans during graded exercise on a treadmill," *Eur. J. Appl. Physiol.*, vol. 70, no. 3, pp. 234–239, 1995.

[10] A. Q. Fischer, B. A. Chaudhary, M. A. Taormina, and B. Akhtar, "Intracranial hemodynamics in sleep apnea," *Chest*, vol. 102, no. 5, pp.1402–1406, 1992.

[11] S. Sun, C. Oliver-Pickett, Y. Ping, A. J. Micco, T. Droma, S. Zamudio, J. Zhuang, S. Y. Huang, R. G. McCullough, A. Cymerman, and L. G. Moore, "Breathing and brain blood flow during sleep in patients with chronic mountain sickness," *J. Appl. Physiol.*, vol. 81, no. 2, pp. 611–618, 1996.

[12] J. He, A. W. Pan, T. Ozaki, Y. Kinouchi, and H. Yamaguchi, "Three channels telemetry system: ECG, blood velocities of the carotid and the brachial arteries," *Biomed. Eng. Appl. Basis Commun.*, vol. 8, no. 4, pp. 364–369, 1996.

[13] D. H. Evans and W. N. McDicken, *Doppler Ultrasound: Physics, Instrumentations and Signal Processing*. New York, NY: Wiley, 2000.

[14] J. A. Jensen, *Estimation of Blood Velocity Using Ultrasound*. New York, NY: Cambridge University Press, 1996.

[15] D. W. Baker, "Pulsed ultrasonic Doppler blood flow sensing," *IEEE Trans. Sonics Ultrason.*, vol. SU-17, no. 3, pp. 170–185, 1970.

[16] C. J. Hartley and J. S. Cole, "Ultrasonic pulsed Doppler system for measuring blood flow in small vessels," *J. Appl. Physiol.*, vol. 37, no. 4, pp. 626–629, 1974.

[17] R. W. Gill and J. D. Meindl, "Low-power integrated circuits for an implantable pulsed Doppler ultrasonic blood flowmeter," *IEEE J. Solid-state Circuits*, vol. SC-10, no. 6, pp. 464–470, 1975.

[18] H. M. Keller, W. E. Meier, M. Anliker, and D. A. Kumpe, "Noninvasive measurement of velocity profiles and blood flow in the common carotid artery by pulsed Doppler ultrasound," *Stroke*, vol. 7, no. 4, pp. 370–377, 1976.

[19] H. V. Allen, J. W. Kutti, and J. D. Meindl, "Integrated circuits for a bidirectional implantable pulsed Doppler ultrasonic blood flowmeter," *IEEE J. Solid-State Circuits*, vol. 13, no. 6, pp. 853–863, 1978.

[20] I. Güler and N. F. Güler, "The electronic detail of a pulsed Doppler blood flow measurement system," *Meas. Sci. Technol.*, vol. 1, no. 10, pp. 1087–1092, 1990.

[21] F. S. Schlindwein, M. J. Smith, and D. H. Evans, "Spectral analysis of Doppler signals and computation of the normalised first moment in real time using a digital signal processor," *Med. Biol. Eng. Comput.*, vol. 26, no. 2, pp. 228–232, 1988.

[22] N. Aydin and D. H. Evans, "Implementation of directional Doppler techniques using a digital signal processor," *Med. Biol. Eng. Comput.*, vol. 32, suppl. 4, pp. S157–S164, 1994.

[23] C. H. Hu, Q. Zhou, and K. K. Shung, "Design and implementation of high frequency ultrasound pulsed-wave Doppler using FPGA," *IEEE Trans. Ultrason. Ferroelectr. Freq. Control*, vol. 55, no. 9, pp. 2109–2111, 2008.

[24] M. Lewandowski, M. Walczak, and A. Nowicki, "Compact modular Doppler system with digital RF processing," in *IEEE Ultrason. Symp. Proc.*, 2009, pp. 1848–1851.

[25] C. H. Hu, K. K. Shung, and A. Chang, "Design of a digital high frequency linear array ultrasound imaging system with high frame rate," in *IEEE Ultrason. Symp. Proc.*, 2007, pp. 1529–1532.

[26] W. D. Richard, D. M. Zar, and R. Solek, "A low-cost B-mode USB ultrasound probe," *Ultrason. Imaging*, vol. 30, no. 1, pp. 21–28, 2008.

[27] X. Xu, L. Sun, J. M. Cannata, J. T. Yen, and K. K. Shung, "High-frequency ultrasound Doppler system for biomedical applications with a 30-MHz linear array," *Ultrasound Med. Biol.*, vol. 34, no. 4, pp. 638–646, 2008.

[28] X. Xu, J. T. Yen, and K. K. Shung, "A low-cost bipolar pulse generator for high-frequency ultrasound application," *IEEE Trans. Ultrason. Ferroelectr. Freq. Control*, vol. 54, no. 2, pp. 443–447, 2007.